Ultra-High-Resolution ^{29}Si Solid-State MAS NMR Investigation of Sorbate and Temperature-Induced Changes in the Lattice Structure of Zeolite ZSM-5

Colin A. Fyfe,*† Harald Strobl, George T. Kokotailo, Gordon J. Kennedy, and Gwyneth E. Barlow

Contribution from the Guelph-Waterloo Centre for Graduate Work in Chemistry, Guelph Campus, Department of Chemistry and Biochemistry, University of Guelph, Guelph, Ontario N1G 2W1, Canada. *Received June 26, 1987*

Abstract: By preparing extremely highly crystalline, highly siliceous samples and careful optimization of all experimental parameters, it is possible to obtain ^{29}Si MAS NMR spectra of zeolite ZSM-5 with line widths of 0.06 ppm (6 Hz) at a proton frequency of 400 MHz, yielding a spectrum for the unloaded form in which up to 21 of the 24 resonances can be observed giving an unambiguous analysis. This ultra-high resolution makes it possible to clearly observe changes induced in the lattice structure by both temperature and the presence of organic sorbates. The change between the monoclinic (24 T -atoms) and orthorhombic (12 T-atoms) forms occurs between 355 and 357 °C and in the case of *p*-xylene at approximately two molecules per 96 T atom unit cell. From the combined effects, the complete three-dimensional phase diagram may be deduced. In the case of acetylacetone, the effects are more complex, there being two low-temperature monoclinic forms in equilibrium with the high-temperature orthorhombic form. These data can be used together with synchrotron-based powder X-ray diffraction studies to obtain a detailed description of the sorbate–lattice interactions in these materials.

Zeolites have been a subject of considerable interest because of their widespread industrial use as catalysts and molecular sieves.[1] Their unique catalytic and sorptive properties arise from their lattice structures which have characteristically very open frameworks containing cavities that are accessible through channel networks. To date, most structural investigations have been by diffraction techniques,[2] but their effectiveness is severely limited in the case of zeolites by the nature of the materials. Thus, although they are very highly crystalline, they are *micro*crystalline (dimensions <10 μm being common), precluding the use of single-crystal diffraction techniques, and structural determinations must be made from the much more limited powder diffraction data.[3,4] In addition, since Si and Al have almost identical scattering factors and are seldom ordered in the zeolite lattice, the distribution of Si and Al within the framework usually cannot be determined by X-ray diffraction.

High-resolution ^{29}Si MAS NMR spectroscopy has recently emerged as a useful and complementary technique to powder X-ray diffraction in the investigation of zeolite structures.[5-7] In the case of low Si/Al ratio materials, the ^{29}Si MAS NMR spectrum shows, to a first approximation, five peaks, corresponding to the five possible local silicon environments Si[4Al], Si[3Al,Si], Si[2Al,2Si], Si[1Al,3Si], Si[4Si] whose relative intensities provide a description of the average *distribution* of Si and Al throughout the lattice.

For the investigation of the lattice structures themselves, it is advantageous to investigate highly siliceous analogues where all of the aluminum atoms have been removed from the lattice while the lattice structure itself can be shown to remain unchanged. The removal of the lattice aluminum yields very narrow ^{29}Si resonances all of which are due to Si[4Si] and which correspond to the crystallographically inequivalent silicon atoms in the unit cell.[8] The numbers and relative intensities of these resonances thus give a direct probe of the lattice structure and are often sensitive to small and subtle changes in the lattice. They have been used to investigate lattice defects and distortions in zeolite ZSM-39,[9] to deduce the correct interpretation of the ^{29}Si spectra of low Si/Al ratio zeolites with multiple lattice sites,[8d,10] and to demonstrate the equivalence of the lattice structures of series of zeolites produced under different synthetic conditions.[11] *It should be emphasized that, in these studies, the NMR and XRD techniques are complementary in nature*, the former being sensitive to local, short-range structure and ordering while the latter monitors long-range ordering and periodicity. Taken together, they provide a more complete description of the lattice structures.

Zeolite ZSM-5 has been of particular interest in recent years because of its high catalytic activity and extreme size and shape selective sorptive properties. It is the best known of a whole family called "pentasils", zeolites that are based on the pentasil building unit composed entirely of five-membered rings shown in Figure

† Department of Chemistry, University of British Columbia, Vancouver, B.C., Canada V6T 1Y6.

(1) (a) Barrer, R. M. *Zeolites and Clay Minerals*; Academic: London, 1978. (b) *Zeolite Chemistry and Catalysis*; Rabo, J. A., Ed.; ACS Monograph 171; American Chemical Society: Washington, DC, 1976. (c) Breck, D. W. *Zeolite Molecular Sieves*; Wiley: New York, 1974.

(2) Meier, W. M.; Olson, D. H. *Atlas of Zeolites Structure Types*; Structure Commission of the International Zeolite Association, 1978.

(3) It has recently been demonstrated that the use of synchrotron X-ray sources permits single-crystal studies to be carried out on much smaller samples. Eisenberger, P.; Newsam, J. B.; Leonowicz, M. E.; Vaughan, D. E. W. *Nature (London)* **1984**, *309*, 45.

(4) The use of Rietveld refinement techniques allows better structural information to be obtained from powder diffraction data. David, W. I. F.; Harrison, W. T. A.; Johnson, M. W. *High Resolution Powder Diffraction*; Materials Science Forum, Catlow, C. R. A., Ed.; Trans. Tech. Publication Andermannsdorf, Switzerland; Vol. 9, pp 89–101.

(5) (a) Lippmaa, E.; Magi, M.; Samoson, A.; Tarmak, M.; Engelhardt, G. *J. Am. Chem. Soc.* **1981**, *103*, 4992. (b) Lippmaa, E.; Magi, M.; Samoson, A.; Engelhardt, G.; Grimmer, A. R. *J. Am. Chem. Soc.* **1980**, *102*, 4889.

(6) (a) Fyfe, C. A.; Thomas, J. M.; Klinowski, J.; Gobbi, G. C. *Angew. Chem.* **1983**, *95*, 257; *Angew. Chem., Intl. Ed. Engl.* **1983**, *22*, 259. (b) Fyfe, C. A.; Kokotailo, G. T.; Kennedy, G. J.; Gobbi, G. C.; DeSchutter, C. T.; Ozubko, R. S.; Murphy, W. J. in *Proceeding of the International Symposium of Zeolites* Elsevier: Science Publishers; held Sept. 3–8, 1984, in Yugoslavia. (c) Kokotailo, G. T.; Fyfe, C. A.; Kennedy, G. J.; Gobbi, G. C.; Strobl, H. J.; Pasztor, C. T.; Barlow, G. E.; Bradley, S.; Murphy, W. J.; Ozubko, R. S. *Pure Appl. Chem.* **1986**, *58*, 1367.

(7) Engelhardt, G.; Michel, D. *High-Resolution Solid State NMR of Zeolites and Related Systems*; John Wiley and Sons: New York, to be published.

(8) (a) Fyfe, C. A.; Gobbi, G. C.; Murphy, W. J.; Ozubko, R. S.; Slack, D. A. *Chem. Lett.* **1983**, 1547. (b) Fyfe, C. A.; Gobbi, G. C.; Murphy, W. J.; Ozubko, R. S.; Slack, D. A. *J. Am. Chem. Soc.* **1984**, *106*, 4435. (c) Klinowski, J.; Thomas, J. M.; Audier, M.; Vasudevan, S.; Fyfe, C. A.; Hartman, J. S. *J. Chem. Soc., Chem. Commun.* **1981**, 570. (d) Fyfe, C. A.; Gobbi, G. C.; Kennedy, G. J.; DeSchutter, C. T. *Chem. Lett.* **1984**, *2*, 163. (e) Thomas, J. M. *J. Mol. Catal.* **1984**, *27*, 59. (f) Thomas, J. M.; Klinowski, J.; Ramdas, S.; Hunter, B. K.; Tennakoon, E. D. B. *Chem. Phys. Lett.* **1983**, *102*, 158.

(9) Kokotailo, G. T.; Fyfe, C. A.; Gobbi, G. C.; Kennedy, G. J.; DeSchutter, C. T. *J. Chem. Soc., Chem. Commun.* **1984**, 1093.

(10) Fyfe, C. A.; Gobbi, G. C.; Kennedy, G. J.; Graham, J. D.; Ozubko, R. S.; Murphy, W. J.; Bothner-By, A. A.; Dadok, J.; Chesnick, A. S. *Zeolites* **1985**, *5*, 179.

(11) Fyfe, C. A.; Kokotailo, G. T.; Strobl, H.; Pasztor, C. S.; Barlow, G.; Bradley, S. *Zeolites*, in press.

0002-7863/88/1510-3373$01.50/0

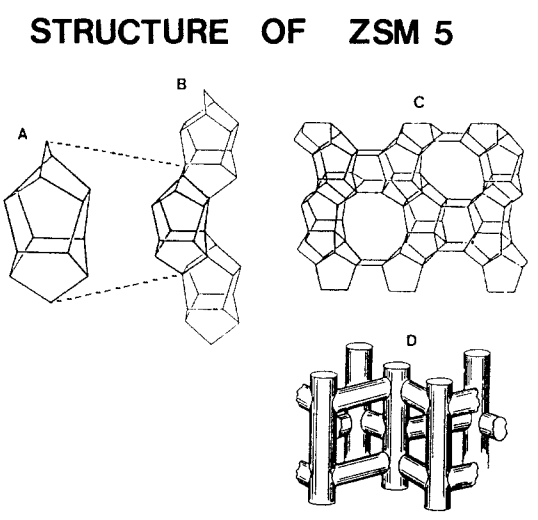

Figure 1. The pentasil building block (A) which forms chains (B) that can be linked to form the skeletal framework of ZSM 5 (C) (the 100 face is shown). The resulting three-dimensional structure has a channel system as indicated schematically (D) after ref 12.

1A. These systems are usually synthesized with an organic "template" cation, $^{+}NR_1R_2R_3R_4$ in the reaction mixture (R_x = C_1–C_2). (The template resides in the cavity after synthesis and may be removed by "calcining", i.e., heating the sample to ~550 °C which decomposes the quaternary salt, evolving NH_3 and oxides and leaving behind H^+ as a hydrated derivative as the positive counterion.) Joining pentasil units into a chain as in Figure 1B and then joining the chains as in Figure 1C yields the lattice structure of ZSM-5.[12] The overall structure of the template-containing form was first deduced from powder diffraction and single-crystal data by Kokotailo and co-workers[12] and has been confirmed by subsequent investigations.[14-16] Tetrapropylammonium–ZSM-5 has apparent orthorhombic symmetry *Pnma* and there are 12 independent T-atoms in the 96 T-atom unit cell. It was also shown that fluoride silicalite, with framework topology the same as that of high silica ZSM-5, is also orthorhombic with space group *Pnma*.[17] On removal of the "loading", the quaternary salt, in a high silica ZSM-5 the framework transforms from orthorhombic to monoclinic symmetry $P_{2_1/n}$ with 24 independent atoms in the unit cell.[18] There is, to date, no complete structure determination of the calcined, monoclinic phase. Previous ^{29}Si MAS NMR investigations of highly siliceous analogues have confirmed that the calcined form has 24 crystallographic T sites in the unit cell[19] and probed the relationship between ZSM-5 and "silicalite"[20] and between ZSM-5 and ZSM-11.[21] It has also been demonstrated qualitatively that changes in the lattice structure could be induced by both temperature and organic molecules[22]

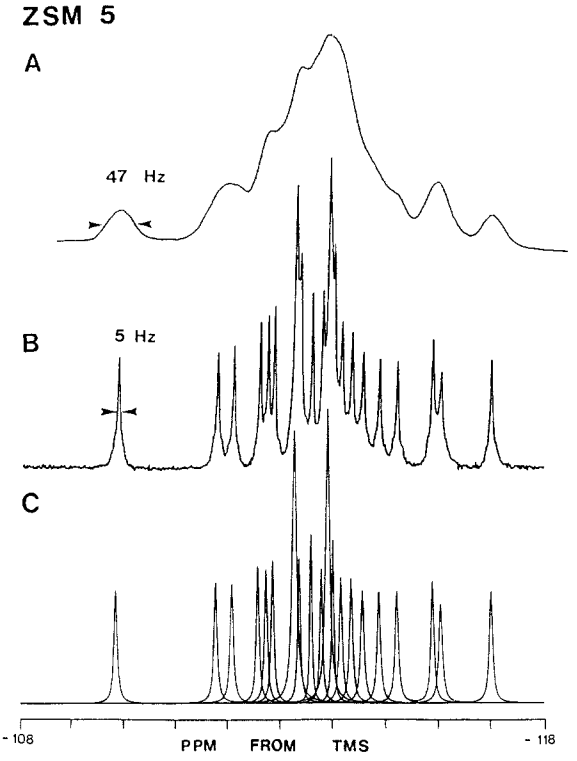

Figure 2. (A) ^{29}Si MAS NMR spectrum of highly siliceous ZSM-5, 79.5 MHz, 6550 scans, 0 Hz line broadening at 295 K from ref 19. (B) ^{29}Si MAS NMR spectrum of very highly siliceous ZSM-5 obtained at 79.5 MHz, 1633 scans, 0 Hz line broadening at 295 K. (C) Individual Lorentzian curves used in the computer simulation of spectrum B.

and an attempt made to define these effects for sorbed xylene and acetylacetone.[23] However, a detailed description of these structural changes has, to date, been precluded by the limited spectral resolution obtainable.

By preparing extremely pure and very highly crystalline samples of completely siliceous ZSM-5 and by carefully optimizing all of the NMR experimental variables, we have recently been able to obtain ultrahigh-resolution ^{29}Si MAS NMR spectra of zeolite ZSM-5 in which 21 of the 24 possible resonances can be clearly resolved, making an unambiguous analysis possible. A preliminary report of this work has been presented.[24] In the present paper we present the results of a detailed investigation of the combined effects of a number of organic molecules and of temperature on the lattice structure of ZSM-5 utilizing this increased spectral resolution in an effort to characterize the system under conditions more comparable to those used in actual catalytic reactions. In a separate and complementary study, we are attempting to investigate these structural changes using diffraction measurements of increased resolution by using a synchrotron X-ray source to collect data on exactly the same systems used for the NMR experiments.[25]

Experimental Section

Samples of high Si/Al ratio ZSM-5 were prepared with tetrapropyl ammonium ion as template and with added ammonium fluoride and ammonium bifluoride. The most highly crystalline products were calcined and hydrothermally dealuminated one or more times at 800 °C for 9 days.

^{29}Si MAS NMR spectra were obtained at 79.6 MHz (proton frequency 400 MHz) on a Bruker high-resolution narrow-bore WH 400 spectrometer.[26] Spinning at the magic angle was achieved by using a modified version of the design by Wind and co-workers[27] with 9 mm o.d.

(12) Kokotailo, G. T.; Lawton, S. L.; Olson, D. H.; Meier, W. M. *Nature (London)* **1978**, *272*, 437.
(13) Olson, D. H.; Kokotailo, G. T.; Lawton, S. L.; Meier, W. M. *J. Phys. Chem.* **1981**, *85*, 2238–2243.
(14) Lermer, H.; Draeger, M.; Steffen, J.; Unger, K. K. *Zeolites* **1985**, *5*, 13.
(15) Chao, K.; Lin, J.; Wang, Y.; Lee, G. H. *Zeolites* **1985**, *6*, 35.
(16) Baerlocher, Ch. *Proceedings of the International Conference on Zeolites, 6th*; Bullerworths: London, 1984; Reno, 1983.
(17) Price, G. D.; Pluth, J. J.; Smith, J. V.; Bennett, J. M.; Patton, R. L. *J. Am. Chem. Soc.* **1982**, *104*, 5971.
(18) Wu, E. L.; Lawton, S. L.; Olson, D. H.; Rohrman, A. C.; Kokotailo, G. T. *J. Phys. Chem.* **1979**, *83*, 2777.
(19) Fyfe, C. A.; Gobbi, G. C.; Klinowski, J.; Thomas, J. M.; Ramdas, S. *Nature (London)* **1982**, *296*, 530.
(20) (a) Fyfe, C. A.; Gobbi, G. C.; Kennedy, G. J. *Chem. Lett.* **1983**, 1551. (b) Thomas, J. M.; Klinowski, J.; Anderson, M. *Chem. Lett.* **1983**, 1555. (c) Fyfe, C. A.; Gobbi, G. C.; Kennedy, G. J. *J. Phys. Chem.* **1984**, *88*, 3248.
(21) Fyfe, C. A.; Kokotailo, G. T.; Kennedy, G. J.; DeSchutter, C. T. *J. Chem. Soc., Chem. Commun.* **1985**, 306.
(22) (a) Fyfe, C. A.; Kennedy, G. J.; DeSchutter, C. T.; Kokotailo, G. T. *J. Chem. Soc., Chem. Commun.* **1984**, 541. (b) West, G. W. *Aust. J. Chem.* **1984**, *37*, 455. (c) Fyfe, C. A.; Kokotailo, G. T.; Lyerla, J. R.; Flemming, W. W. *J. Chem. Soc., Chem. Commun.* **1985**, 740. (d) Hay, D. G.; Jaeger, H.; West, G. W. *J. Phys. Chem.* **1985**, *89*, 1070.
(23) Kennedy, G. J. Ph.D. Thesis, University of Guelph, 1984.
(24) Fyfe, C. A.; O'Brien, J. H.; Strobl, H. *Nature (London)* **1987**, *363*, 6110.
(25) Cox, D.; Kokotailo, G. T.; Fyfe, C. A.; and co-workers, work in progress.
(26) Fyfe, C. A.; Gobbi, G. C.; Hartman, J. S.; Lenkinski, R. E.; O'Brien, J. H.; Beange, E. R.; Smith, M. A. R. *J. Magn. Reson.* **1982**, *47*, 168.

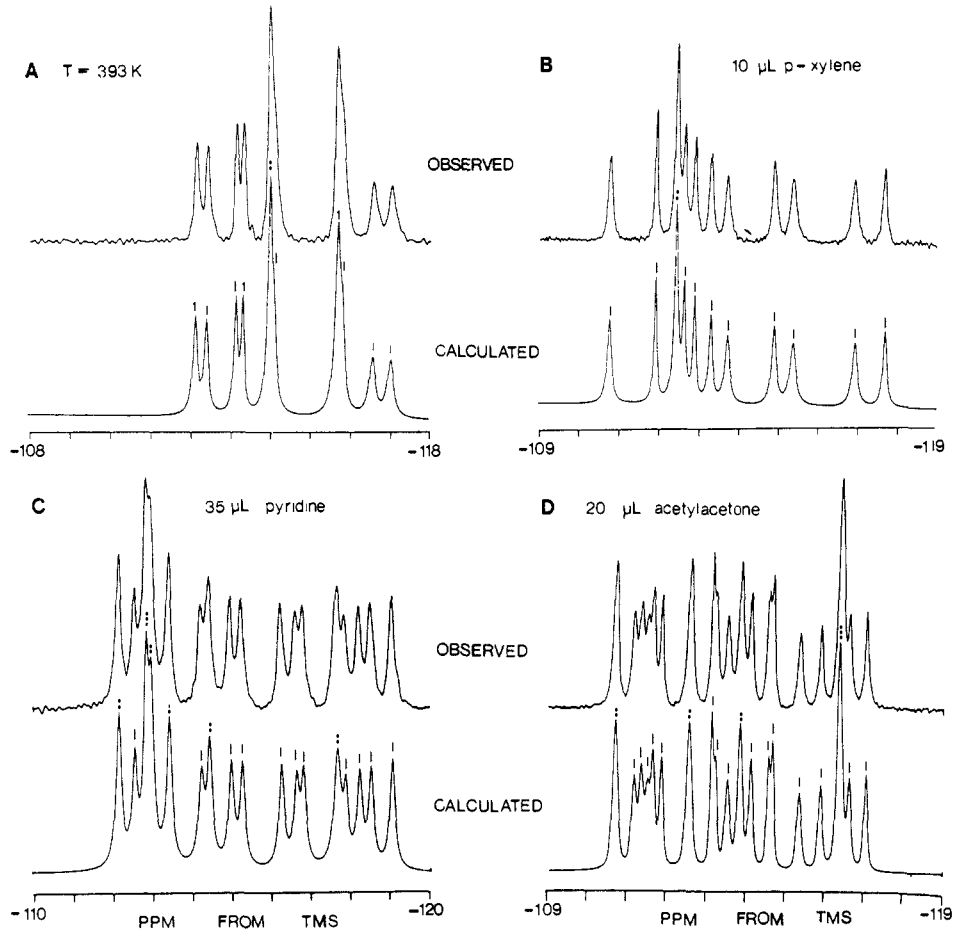

Figure 3. (A) ^{29}Si MAS NMR spectrum of highly siliceous ZSM-5 at 393 K (120 °C), 1225 scans, with a simulation of the experimental spectrum in terms of 12 Lorentzian curves of equal intensity. (B) ^{29}Si MAS NMR spectrum of highly siliceous ZSM-5 at 295 K (22 °C) obtained after the addition of 10 μL of *p*-xylene per 250 mg (approximately 2 molecules per unit cell) and a simulation of the experimental spectrum in terms of 12 Lorentzian curves of equal intensity. The relative intensities are indicated above the peaks. (C) ^{29}Si MAS NMR spectrum of highly siliceous ZSM-5 at 295 K (22 °C) obtained after the addition of 35 μL of pyridine per 250 mg (approximately 10 molecules per unit cell) and a simulation of the experimental spectrum in terms of 24 Lorentzian curves of equal intensity. The relative intensities are indicated above the peaks. (D) ^{29}Si MAS NMR spectrum of highly siliceous ZSM-5 at 295 K (22 °C) obtained after the addition of 20 μL of acetylacetone per 250 mg (approximately 4.5 molecules per unit cell) and a simulation of the experimental spectrum in terms of 24 Lorentzian curves of equal intensity. The experimental spectra B, C, and D were obtained in 5500 scans at 79.5 MHz with 0 Hz line broadening.

cylindrical spinners of Torlon operating at 4–6 kHz. The magic angle was set by using the ^{79}Br resonance of KBr mixed with the sample.[28] Variable-temperature MAS measurements were automated by using a standard Bruker variable-temperature controller.

Powder XRD patterns were obtained with use of a Rigaku diffractometer and the sorbate loaded samples were protected by a covering of an amorphous collodian film during data collection. NMR spectra were obtained both before and after the XRD measurements to ensure sample integrity.

Results and Discussion

General. Figure 2 illustrates the ultrahigh resolution that can be obtained with this system. The line widths are approximately 5 Hz (~0.06 ppm) which is an improvement of an order of magnitude over the original spectra reported for this material. Of the 24 postulated resonances 20 are clearly observed, making a deconvolution of the spectrum straightforward as shown. It should be emphasized that *no resolution enhancement* has been used on the data and use of such techniques or alternative transformation procedures will yield even more highly resolved spectra. Resonances as narrow as these have not been reported to date for *any* rigid crystalline materials, and it may be that optimization of sample preparation and experimental techniques could lead to similar improvements in the solid-state NMR spectra of other systems.

As can be seen from Figure 3, this resolution is largely maintained both at elevated temperatures and in the presence of sorbed organic molecules. There is a small additional contribution to the line widths as a different sample was used from that shown in Figure 2, the particular material being chosen because its small crystallite size (1 μm^3) is optimal for the synchrotron X-ray diffraction experiments. The limiting high-temperature spectrum (120 °C, Figure 3A) can be deconvoluted in terms of 12 sites of equal intensity, as can that of the *p*-xylene loaded sample where all twelve resonances can be observed (Figure 3B). However, the spectra of the acetylacetone and pyridine loaded materials deconvolute in terms of 24 T-atom unit cells (Figure 3C,D). Although, as indicated in the introduction, induced spectral changes have been previously detected, the resolution was not sufficient to make the above assignments unambiguously.[22d,e] The relationships between these different effects are complex and for clarity of presentation will be discussed in detail in separate sections. The criteria which will be used to separate the different contributions to the observed spectral changes are that, in general, lattice expansions and changes in dielectric would be expected to produce gradual changes in the spectra, while a phase change to a new lattice structure is more likely to be reflected in an abrupt, discrete spectral change.

Effect of Sorbed *p*-Xylene. The effect of sorbed *p*-xylene at ambient temperature on the ^{29}Si MAS NMR spectrum is shown in Figure 4. At very low loadings (~2 μL/250 mg or 0.4 molecule per unit cell) there is little effect on the spectrum except for small, gradual shifts in individual resonances. The fact that

(27) Wind, R. A.; Anthonio, F. E.; Duijvestijn, M. J.; Schmidt, J.; Trommel, J.; deVette, C. M. C. *J. Magn. Reson.* **1983**, *52*, 424.
(28) Frye, J. S.; Maciel, G. E. *J. Magn. Reson.* **1982**, *48*, 125.

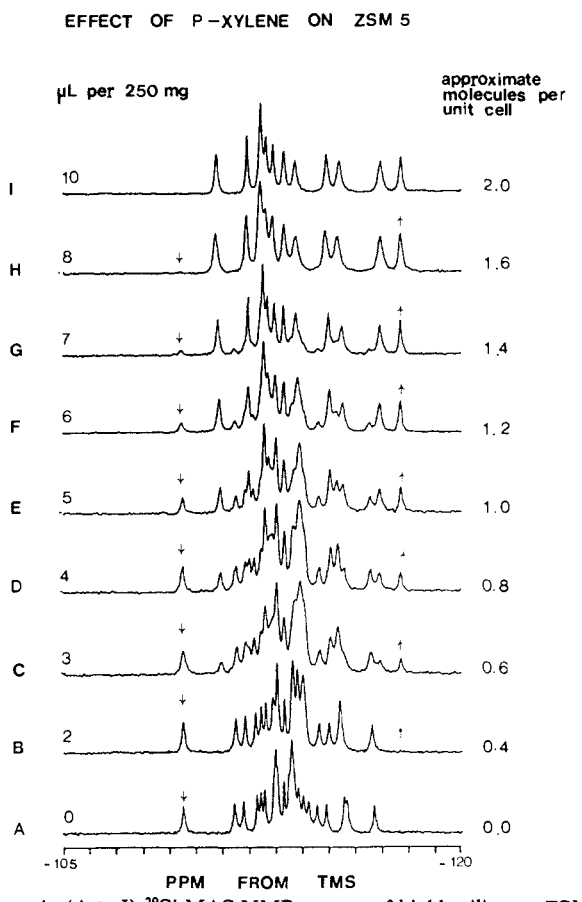

Figure 4. (A to I) ^{29}Si MAS NMR spectra of highly siliceous ZSM-5 loaded with increasing amounts of *p*-xylene as indicated. Spectra were obtained at 295 K at 79.5 MHz (9.4 T) with 500 scans and 0 Hz line broadening. The ↓ symbol shows the disappearance of a resolved characteristic of the monoclinic symmetry (24 T sites per unit cell) while the ↑ symbol indicates the appearance of one characteristic of the orthorhombic symmetry (12 T sites per unit cell).

they occur, however, indicates that some *p*-xylene is present in the structure corresponding to the "unchanged" spectrum. At loadings greater than 8 μL/250 mg of sample or 1.6 molecules per unit cell, the spectrum shows only 12 resonances of equal intensity, clearly indicating a change in the unit cell symmetry, in agreement with the powder XRD data where the collapse of the characteristic "doublet" at $2\theta \simeq 24.4°$ to a single reflection has been interpreted in terms of a change from monoclinic to orthorhombic symmetry.[22a]

At intermediate loadings of *p*-xylene, the resonances all remain sharp, indicating that all of the material being examined remains highly ordered and crystalline at all stages. The spectra show that both the high- and low-symmetry forms of ZSM-5 forms are present at these intermediate loadings in different proportions. The arrows in the figure indicate the changing relative intensities of some of the better resolved resonances of the two forms. The midpoint of the transition, where equal proportions of the two forms are present, corresponds roughly to one molecule per 96 T-atom unit cell and the change is complete when two molecules have been added.

The transition from one form to the other is a smooth "S" shaped curve as shown in bold outline at the front of the three-dimensional phase diagram in Figure 8 with the actual experimental points plotted. By selectively inverting a single resolved resonance with a DANTE pulse sequence[29] and probing the subsequent spectra after varying time intervals, it can be shown that there is no detectible interconversion between the two forms on a time scale of several seconds.

The sharpness of the resonances of both spectra indicate that the individual phases exist over substantial volumes, perhaps even

(29) Morris, G. A.; Freeman, R. *J. Magn. Reson.* **1978**, *29*, 433.

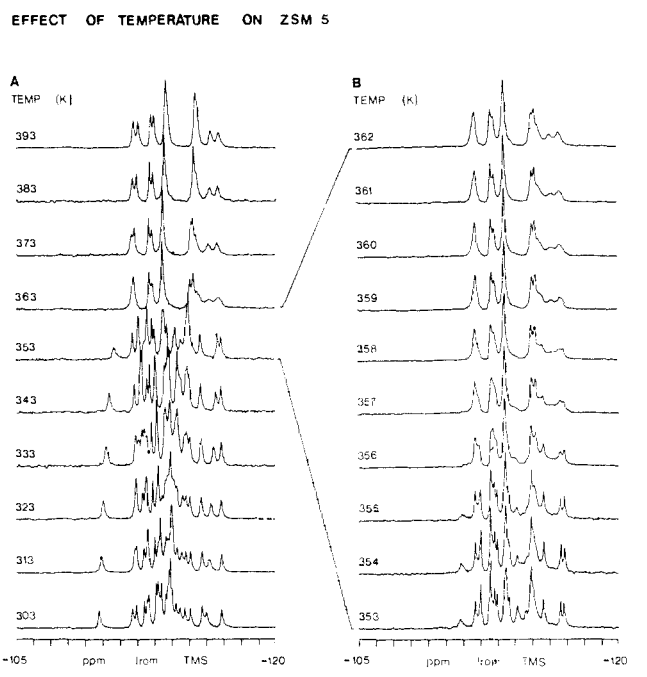

Figure 5. (A) ^{29}Si MAS NMR spectra of highly siliceous ZSM-5 obtained at 10-deg intervals between 303 and 393 K (30 to 120 °C) as indicated. The spectra were obtained at 79.5 MHz (9.4 T) with 500 scans and 0 Hz line broadening. (B) ^{29}Si MAS NMR spectra of highly siliceous ZSM-5 obtained at 1-deg intervals between 353 and 363 K (80 and 89 °C). The spectra were obtained at 79.5 MHz (9.4 T) with 500 scans and 0 Hz line broadening.

over whole crystallites, but the NMR data cannot determine quantitatively their extent.

Effect of Temperature. Figure 5A shows the detailed temperature dependence of the ^{29}Si MAS NMR spectra of highly siliceous ZSM-5 recorded at 10-deg intervals. From the solid-state NMR spectra of materials of this type the resonances are relatively sharp in all of the spectra, indicating that the material again remains crystalline at all stages. Again, the spectra are in general agreement with those previously published, but the limited resolution of the latter precluded detailed interpretation.[22c,d] At low temperatures, between 303 and 333 K, there are only gradual shifts in the resonances (of which the most marked is indicted by the dashed line), most probably reflecting the gradual expansion of the lattice and corresponding small changes in local geometries of the T atoms. Between 333 and 353 K there is some broadening of the resonances most evident in the lowest field signal at δ −107.7, suggesting that the lattice is becoming somewhat distorted, and then between 353 and 363 K there is an abrupt change to a quite different spectrum with twelve resonances due to a change in the lattice structure. Spectra obtained at 1-deg intervals with careful temperature control indicate that the conversion between the 24 resonance and 12 resonance forms occurs between 355 and 357 K for this sample (Figure 5B) which may reflect the limit determined by temperature gradients over the sample volume.

The spectrum now shows only gradual shifts as the temperature is raised further although the resonances, particularly those at high field (δ −116 to −117.0), gradually narrow, indicating that the structure is becoming more highly ordered. As demonstrated earlier (Figure 3) the limiting spectrum can be deconvoluted in terms of a 12 independent silicon atom unit cell, in agreement with the powder XRD data of Hay and co-workers[22d] which showed the transformation of the two characteristic reflections at $2\theta = 24.4°$ into a single reflection from which they deduced the symmetry of the high-temperature form to be orthorhombic. However, the previous NMR data were interpreted in terms of a 24 inequivalent silicon unit cell.[22d] Spectra obtained at increasing tempertures followed immediately by duplicate spectra at decreasing temperatures are identical, indicating that there is no hysteresis within ±2 deg error on the time scale of the experiment, approximately 35 min at each temperature.

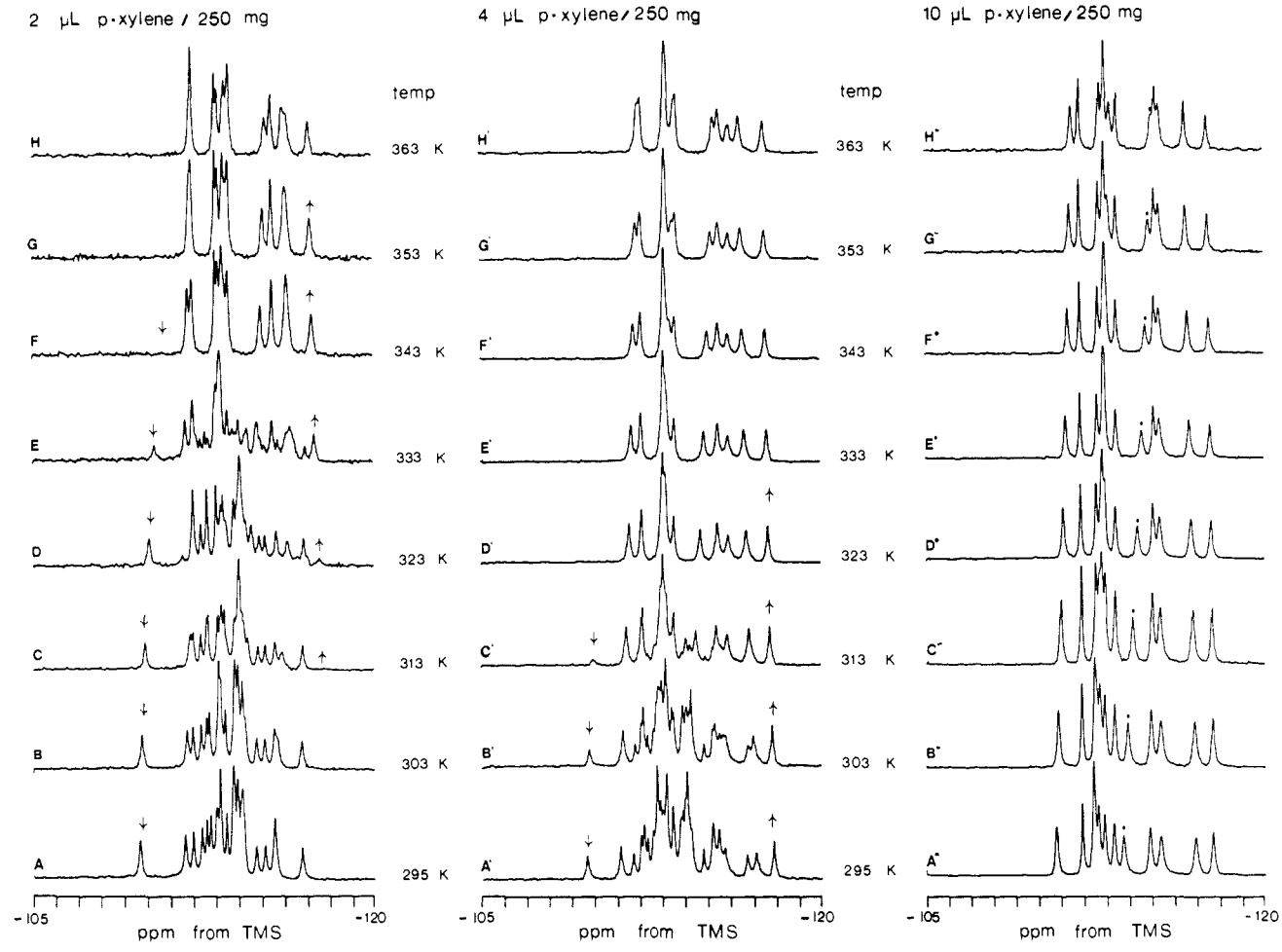

Figure 6. ^{29}Si MAS NMR spectra of highly siliceous ZS-5 obtained by varying both the temperature in 10-deg intervals between 295 to 363 K (22 to 90 °C) and the concentration of *p*-xylene (2, 4, and 10 μL of *p*-xylene per 250 mg of ZSM-5). All spectra were obtained at 79.5 MHz (9.4 T) with 500 scans and 0 Hz line broadening. The arrows above spectra A to H and A′ to H′ indicate the disappearance (↓) of the monoclinic form (24 T sites per unit cell) and the appearance (↑) of the orthorhombic form (12 T sites per unit cell). The dots above one of the peaks in the spectra A″ to H″ indicate the gradual chemical shift which occurs due to general lattice expansions and dielectric changes for the resonance most sensitive to these effects.

Combined Effects of Temperature and Sorbed *p*-Xylene. The combined effects of temperature and sorbed *p*-xylene have been investigated for a number of different *p*-xylene concentrations. The effect of temperature depends on the concentration of *p*-xylene, and spectra characteristic of the two different types of behavior are presented in Figure 6. At low loadings of *p*-xylene, the effect of the organic sorbate is to lower the temperature range over which the transition to the high-temperature phase takes place. During the transition, both low- and high-temperature forms co-exist as indicated by the arrows in the figure, and all of the material is crystalline at all stages. Above the transition, there are only minor and gradual shifts in the resonances reflecting expansion of the lattice, and the high-temperature spectra are all consistent with a 12 independent silicon unit with the peaks occurring in three groupings of relative intensities 2:5:5, similar to that of the high-temperature spectrum of the unloaded material (Figure 2A). Similar experiments on a series of samples with different loadings of *p*-xylene indicate that the transition temperature is gradually lowered as the concentration of *p*-xylene is increased.

At a *p*-xylene concentration high enough to produce exclusively the 12 resonance spectrum (10 μL/250 mg), only gradual changes in the shift values of the resonances occur with temperature reflecting the effects of lattice expansion. At all temperatures, there is only one phase present, and the material in the sample is crystalline at all stages.

Effect of *p*-Xylene at Elevated Temperatures. All of the samples have high-temperature spectra consisting of 12 resonances of equal intensities in a general arrangement of three groupings of relative intensities 2:5:5. The details of the relationship between them

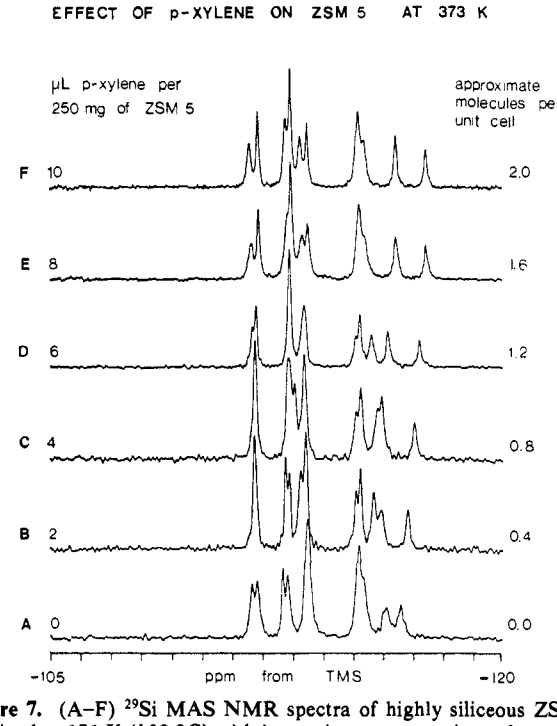

Figure 7. (A–F) ^{29}Si MAS NMR spectra of highly siliceous ZSM-5 obtained at 373 K (100 °C) with increasing concentrations of *p*-xylene. The spectra were obtained at 79.5 MHz (9.4 T) with 500 scans and 0 Hz line broadening.

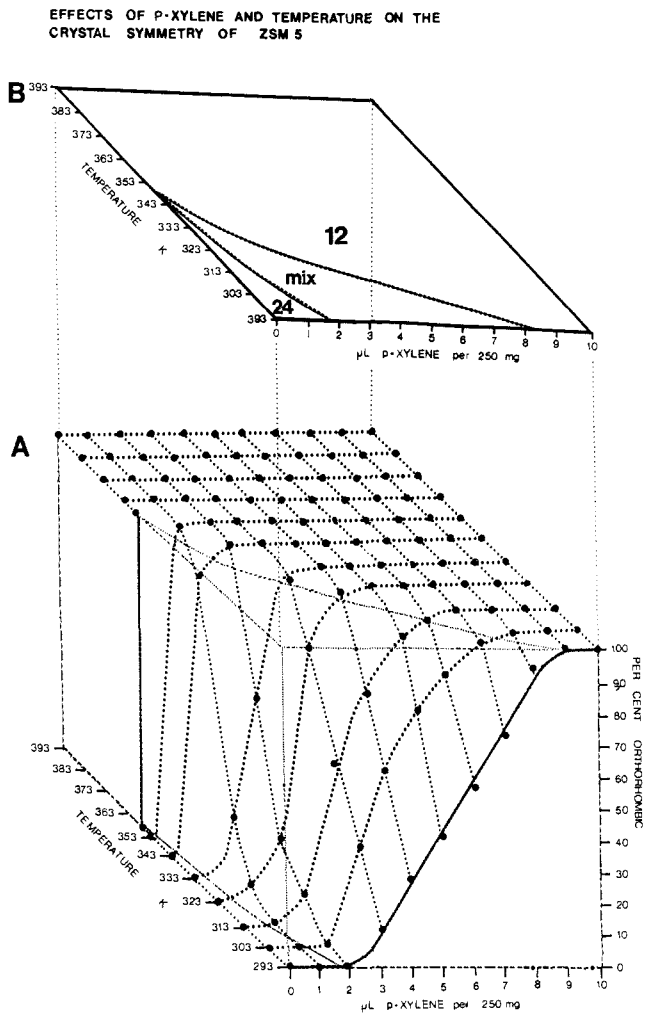

Figure 8. (A) A three-dimensional surface of the crystallographic phase relationship between the concentration of *p*-xylene (increasing left to right) and temperature (increasing front to back). The vertical axis gives the percent of the orthorhombic (12 crystallographically inequivalent T sites in the unit cell) phase present. The solid line going left to right shows the effect of increasing *p*-xylene concentration upon the crystal symmetry at ambient temperature (cf. Figure 4). The near vertical solid line at 355 K shows the effect of temperature on an unloaded ZSM-5 sample (cf. Figure 5). The solid circles are selected experimental results from the MAS NMR data, and the dotted curves joining them show variation with *p*-xylene concentration at constant temperature (left to right) and variation with temperature at constant *p*-xylene concentration (front to back). (B) A two-dimensional projection of part A as indicated showing the relationship of the orthorhombic and monoclinic crystallographic phases with varying temperature and concentration of *p*-xylene.

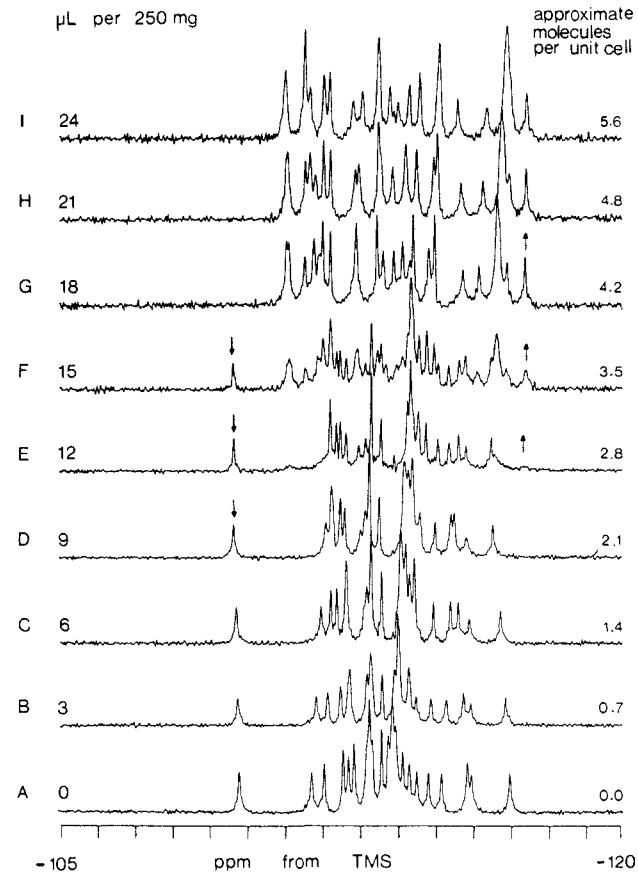

Figure 9. (A–I) ^{29}Si MAS NMR spectra of highly siliceous ZSM-5 loaded with increasing amounts of acetylacetone. The spectra were obtained at 295 K at 79.5 MHz (9.4 T), with 1000 scans and −5 Hz (0.6 GB) resolution enhancement. The symbols (↓) and (↑) indicate the disappearance and appearance of resonances characteristic of the two forms.

can be seen from Figure 7 which shows the effect of increasing the *p*-xylene concentration at a fixed temperature of 100 °C. There are complex and quite substantial shifts in the positions of the resonances but, as indicated by the dashed lines, these are gradual and a function of the *p*-xylene concentration and only a single lattice symmetry exists throughout the series. The changes could be due in part to changes in the local dielectric but are probably mainly due to changes in the lattice dimensions as the number of organic molecules in the cavities increases, but with no change in the lattice symmetry.

Relationship between the Phases. The general conclusions derived from all of the spectral data discussed above are summarized in the "phase diagram" shown in Figure 8. It appears that two discrete structures exist for the ZSM-5 as a function of the combined effects of temperature and sorbed *p*-xylene. In the low-temperature, low-concentration range, the unit cell has 24 crystallographically inequivalent T sites of equal occupancy, while in the high-temperature, high-sorbate concentration domain the unit cell contains 12 crystallographically inequivalent T sites, again of equal occupancy. This is in agreement with the general conclusions from previous XRD data where a transition from monoclinic to orthorhombic symmetry was postulated although it should be noted that the NMR data taken alone cannot distinguish between a static structure of real higher symmetry and a dynamic structure giving an apparent increase in symmetry due to spectral averaging. A complete description of the structures, including the location of the organic sorbates, should result from synchrotron-based XRD investigations of exactly the same systems studied by NMR using the data of Figure 9 to choose the most appropriate temperature/concentration combinations.

The Combined Effects of Temperature and Acetylacetone. As will be seen, the situation with acetylacetone (acac) as sorbate is similar to, but more complex than that discussed above for *p*-xylene. For conciseness and clarity of presentation, the data will be discussed in exactly the same sequence used for *p*-xylene.

Figure 9 shows the effect of gradually increasing the concentration of acac. Between 12 and 18 μL/250 mg, the NMR spectra indicate that two distinct lattice structures exist as indicated by the arrows, with only one phase at higher loading levels. In contrast to the situation with *p*-xylene, however, there are still 24 crystallographically inequivalent silicons in the new limiting structure. Previous spectra were not of high enough resolution to detect this difference in behavior. Corresponding powder XRD measurements show that the reflections at $2\theta \simeq 24.4°$ change to a single reflection, indicating a change in structure, but its width suggests that the change to higher symmetry is not complete, in agreement with the NMR data.

Figure 10 shows a typical example of the effect of temperature on the ^{29}Si MAS NMR spectrum at low loadings of acac. There is a clear transition between 323 and 343 K with both low- and high-temperature forms completely crystalline and coexisting. As in the case of *p*-xylene, the high-temperature spectrum consists

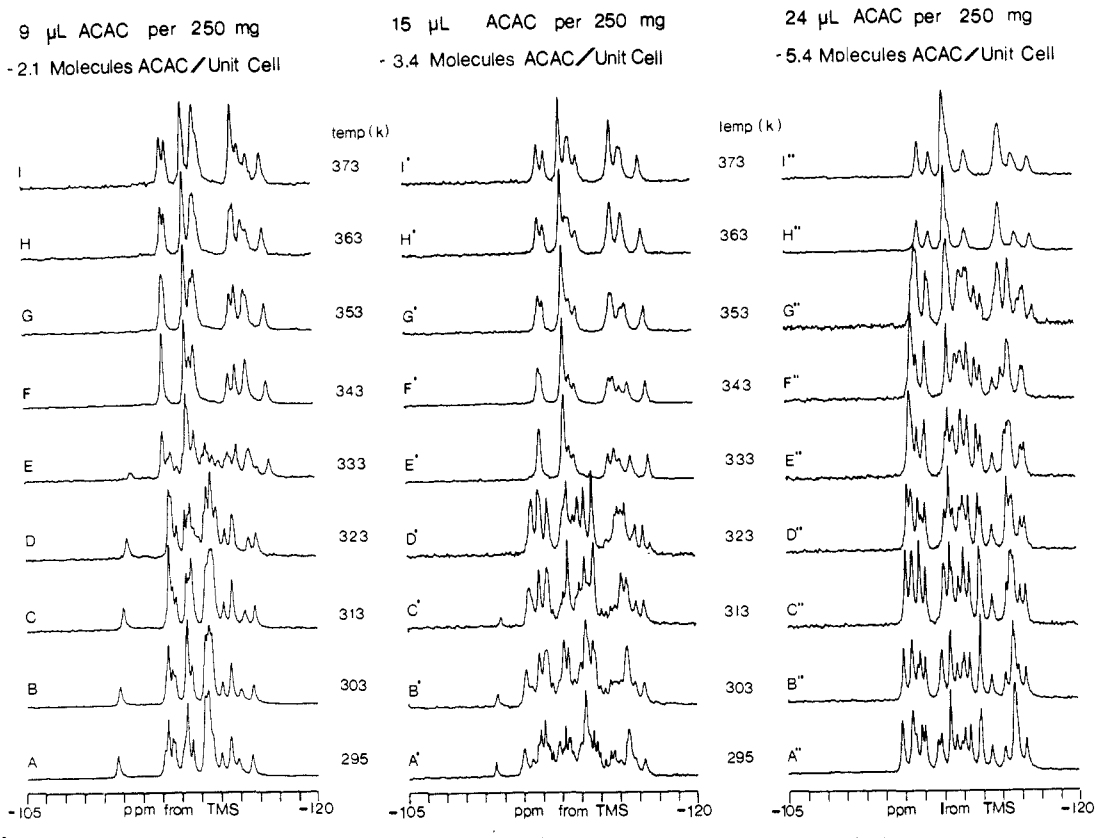

Figure 10. ^{29}Si MAS NMR spectra of highly siliceous ZSM-5 obtained by varying both the temperature in 10-deg intervals between 295 to 363 K and the concentration of acetylacetone (9, 15, 24 μL of AcAc per 250 mg of ZSM 5). All spectra were obtained at 79.5 MHz (9.4 T) with 500 scans and 0 Hz line broadening.

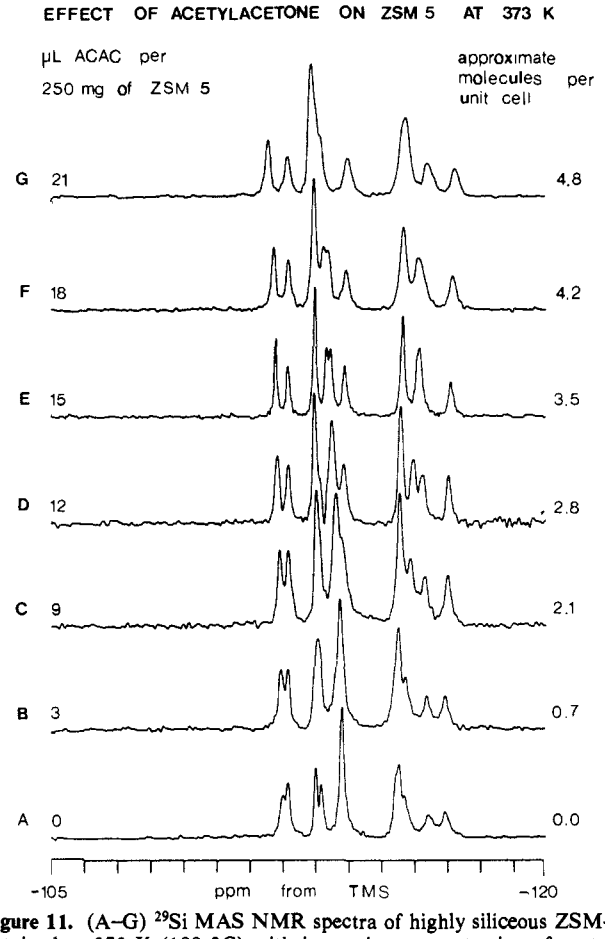

Figure 11. (A–G) ^{29}Si MAS NMR spectra of highly siliceous ZSM-5 obtained at 373 K (100 °C) with increasing concentration of acetylacetone. The spectra were obtained at 79.5 MHz (9.4 T) with 500 scans and 0 HZ line broadening.

of 12 resonances in the three characteristic groupings of relative intensities 2:5:5. Studies of a series of samples with different but low acac concentrations indicate that there is a consistent decrease in the transition temperature with increasing acac concentration.

At high acac loadings, where only the high sorbate 24 T site phase is present, Figure 10 shows that increasing the temperature again induces a change to a 12-resonance pattern; however, the transition temperature is now higher (333–353 K) compared to that of the low loading, indicating a different mechanism for the transition. The temperature dependence at intermediate loadings of acac clearly shows that there is a small composition/temperature range in which all three lattice structures can co-exist.

Figure 11 shows the effect of increasing the acac concentration at high temperatures (100 °C). As in the case of *p*-xylene, only gradual changes occur in the resonance positions indicating that a single phase exists, characterized by a unit cell with 12 crystallographically inequivalent silicons. The similarities in the positions and groupings (2:5:5) of the resonances to those for *p*-xylene suggest that the basic lattice structure and symmetry is the same in both cases with minor differences induced by the particular sorbate.

All of the data for this system can be summarized as before in the "phase diagram" of Figure 12 which shows the presence and ranges of stability of the three lattice structures distinguishable by NMR.

Effect of Other Sorbates. Nature of the Induced Structural Changes. Other sorbates show various types of behavior. Thus, the addition of dimethyl sulfoxide (DMSO) induces a change to a 12-line spectrum as does *p*-xylene while toluene and pyridine give 24-line patterns similar to that described for acac. The addition of benzene yields a new 24-line pattern over a small concentration range transforming to a 12-line spectrum at higher loadings, the most complex behavior observed to date. A possible explanation may be that the "three species" behavior of acac may be the general case, of which the "two species" behavior of *p*-xylene is a special case where the stability field of the high-sorbate 24-line form is not accessible at ambient temperatures. In all cases, to

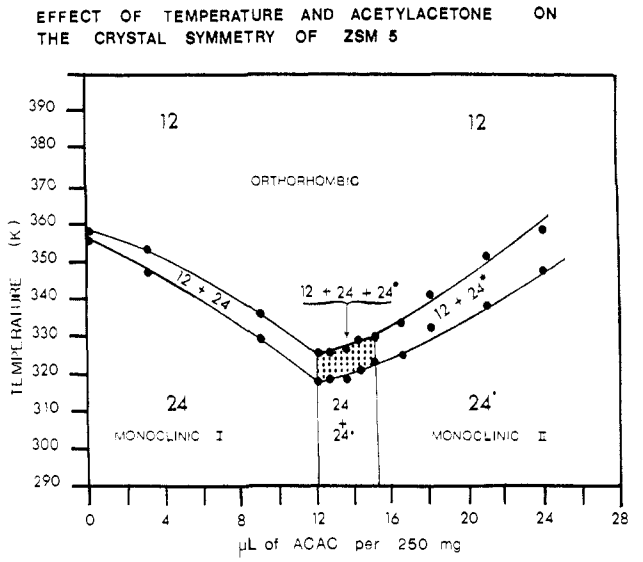

Figure 12. Phase diagram showing the relationship between the three observed phases (monoclinic I, monoclinic II and orthorhombic) with variation of temperature and the concentration of acetylacetone. All three phases coexist in the central region of the diagram.

a greater or lesser degree, the powder diffraction data show the loss of the two reflections at $2\theta \simeq 24.4°$. However, the XRD pattern is an average and reflects mainly the lattice periodicity and may not be sensitive enough to detect that the symmetry of the combination of lattice plus sorbates may be lower than that of the lattice alone. In some other situations involving lattice and site symmetry effects, the high-resolution solid-state NMR spectra have been more sensitive to local symmetry than have diffraction measurements.

What is clear, is that the ZSM-5 lattice structure undergoes changes to accommodate sorbed organic molecules and that the details of the change reflect both the nature and the concentration of the sorbed organics at a given temperature. Using the "phase diagrams" of Figures 8 and 12 as guides, we have initiated structural studies of the various unloaded and loaded forms of this zeolite lattice at selected temperatures. The use of synchrotron-based X-radiation should not only provide data of sufficient accuracy to detail the changes in lattice structures, known from preliminary experiments to involve relatively small changes in cell dimensions and angles, but should also allow the prefered sites which the organics occupy within the unit cell to be determined. From these complementary techniques, it is anticipated that a full understanding of this phenomenon at the molecular level will emerge. It should be noted that these effects are by no means universal. The only other zeolite system in which we have observed them to date is the closely related ZSM-11, and they may possibly be related to the very versatile nature of ZSM-5 as a catalyst.

Acknowledgment. The authors acknowledge the financial support of the Natural Sciences and Engineering Research Council of Canada in the form of an Operating Grant (CAF) and Graduate Scholarships (H.S. and G.J.K.). They also acknowledge the Alexander von Humboldt Senior Scientist Award (G.T.K.).

Registry No. *p*-Xylene, 106-42-3; acetylacetone, 123-54-6; pyridine, 110-86-1; dimethyl sulfoxide, 67-68-5; toluene, 108-88-3; benzene, 71-43-2.

Intermolecular Hydrogen-Bonding Effect on ^{13}C NMR Chemical Shifts of Glycine Residue Carbonyl Carbons of Peptides in the Solid State

Shinji Ando,[†] Isao Ando,*[†] Akira Shoji,[‡] and Takuo Ozaki[‡]

Contribution from the Department of Polymer Chemistry, Tokyo Institute of Technology, Ookayama, Meguro-ku, Tokyo, Japan 152, and Department of Industrial Chemistry, College of Technology, Gunma University, Tenjin-cho, Kiryu-shi, Gunma, Japan 376.
Received August 6, 1987

Abstract: In order to investigate the effect of hydrogen bonding on the ^{13}C NMR chemical shifts of carbonyl carbons in peptides in the solid state, ^{13}C CP/MAS NMR spectra were measured for a series of the oligopeptides containing glycine residues, of which the crystal structures were already determined by X-ray diffractions. It was found that the ^{13}C chemical shifts of the carbonyl carbons in the >C=O···H—N< type hydrogen bond form move downfield with a decrease in the hydrogen bond length but those in the >C=O···H—N^+< type hydrogen bond form move upfield with a decrease in the hydrogen bond length. Further, the ^{13}C chemical shift behavior of the carbonyl carbon of polyglycine with forms I and II was reasonably explained in terms of the difference in their hydrogen bond lengths. The quantum chemical calculation of the ^{13}C shielding constant for the model compounds was done and reproduced reasonably the experimental results taking into account the hydrogen bond and conformational effects.

Most recently, we have reported that the isotropic ^{13}C chemical shifts (σ_{iso}) and the principal values of ^{13}C chemical shift tensors (σ_{11}, σ_{22} and σ_{33}) for carbonyl carbon of the glycine residues (Gly CO) incorporated into some homopolypeptide chains such as poly(L-alanine), poly(β-benzyl-L-aspartate), etc., are significantly displaced depending on their conformational changes, as determined by the cross polarization–magic angle spinning (CP-MAS) technique.[1] It is also noted that the magnitude of the chemical shift tensor displacement is larger for σ_{22} (the midfield component) and σ_{33} (the upfield component) than σ_{iso}. The fact that the direction of the conformation-sensitive component σ_{22} is the same as that of the C=O bond suggests that the signal position of Gly

[†] Tokyo Institute of Technology.
[‡] Gunma University.

(1) Ando, S.; Yamanobe, T.; Ando, I.; Shoji, A.; Ozaki, T.; Tabeta, R.; Saitô, H. *J. Am. Chem. Soc.* **1985**, *107*, 7648.

0002-7863/88/1510-3380$01.50/0